J. Phys. A: Math. Gen. 27 (1994) 1453–1462. Printed in the UK

Reaction kinetics beyond rate equations: a correlation-function study of the effects of space dimension and reactant mobilities on the bimolecular annihilation reaction

E Kotomin†‡, V Kuzovkov†, W Frank‡§ and A Seeger‡§

† University of Latvia, Institute of Solid State Physics, 19 Rainis Blvd., Riga LV 1050, Latvia

‡ Max-Planck-Institut für Metallforschung, Institut für Physik, Heisenbergstraße 1, D-70569 Stuttgart, Federal Republic of Germany

§ Universität Stuttgart, Institut für Theoretische und Angewandte Physik, Stuttgart, Federal Republic of Germany

Abstract. A novel correlation-function approach, making use of many-particle densities and terminating their hierarchy by employing Kirkwood's superposition principle, is applied to the bimolecular annihilation reaction $A+B\rightarrow 0$. The roles of initial concentrations, space dimension and ratio of the reactant diffusivities in the modification of the reaction rate by many-particle effects are compared with computer simulations. The many-particle effects cause the reaction $A+B\rightarrow 0$ to exhibit spatial self-organization phenomena even in the absence of direct A–A or B–B interactions. It is argued that this result casts serious doubts on the validity of the Hanusse–Tyson–Light theorem in synergetics.

1. Introduction

The theoretical treatment of the kinetics of diffusion-controlled reactions is usually based on rate equations for the spatially averaged concentrations of the reaction partners and on the law of mass action, by and large with satisfactory results [1]. These are clearly limitations of this approach, which disregards the fluctuations in the concentrations of the reactants, but only recently has the interest in them become widespread [2–9]. Starting with the pioneering work of Ovchinnikov and Zeldovich [10] it has been gradually realized [11–13] that reaction-induced fluctuations in the density of the reactants can give rise not only to deviations from the time laws predicted by the standard approach [1] but also to the formation of patterns consisting of alternating domains of the reacting species A and B (in the following called 'particles'). This constitutes an example of self-organization by 'chemical' reactions, a field extensively investigated in synergetics [14, 15] though mainly on meso- or macroscopic spatial scales and quite often on fairly complicated systems [16].

The present paper deals with the case in which the driving force for self-organization arises from the annihilation of particles A with their antiparticles B according to the bimolecular reaction

$$A+B\rightarrow 0. \tag{1}$$

Here self-organization is a universal phenomenon as indicated by the fact that it may occur not only in diffusion-controlled reactions [14, 17–19] but also in tunnelling

0305-4470/94/051453+10$19.50

reactions [20–22] and in the case of the accumulation of immobile lattice defects under low-temperature irradiation [4, 23, 24]. The practical importance of the self-organization effects in annihilation reactions is illustrated by the observation that in the last-mentioned case the defect concentration may exceed the saturation concentration obtained for a random defect distribution by factors 3 or 4 [25–27].

The existence of the self-organization phenomena referred to above has been demonstrated both by electron-microscopy work and computer simulation. Nevertheless, important issues have remained open, among them the dependence on the space dimension $d(=1, 2$ or $3)$ of the system and on the relative diffusivities $\kappa = D_A/D_B$ of the reactants. (Note, for example, that the diffusivities D_A and D_B appear in the rate-equation formulation only through the 'effective diffusivity' $D = D_A + D_B$, whereas intuitive arguments indicate that the self-organization phenomena should differ considerably in the limiting cases $\kappa = 0$ and $\kappa = 1$.) On some questions, the literature contains conflicting statements; e.g. a scaling approach [28–30] has confirmed the occurrence of particle segregation in the presence of a particle source for $d = 1$ and 2 but not for $d = 3$. Linear stability analysis of the same problem [31] predicts that segregation of particles of different kind occurs only under intensive irradiation and for mobile interacting particles, which is at variance with results of computer simulations [2–4].

The fact that different approaches (for details see [2–4]) lead to confusing if not conflicting results may be traced to a common weakness, namely their *mesoscopic* character. This makes them insensitive to effects on the *microscopic* scale that becomes relevant when the domain sizes shrink to a few interatomic distances while the systems remain mesoscopically homogeneous.

2. Description of many-particle effects by correlation functions

This paper considers many-particle effects in the kinetics of the reaction (1) using a microscopic approach originally developed in order to analyse the roles of the dimension of space and of the relative mobilities of the reactants [2, 32, 33]. The basic quantities are the macroscopic concentrations $n_A(t)$ and $n_B(t)$ (which, for simplicity, are assumed to be equal initially and to remain so during all times t) and the correlation functions $X_A(r, t)$, $X_B(r, t)$ and $Y(r, t)$ describing the joint correlations between A particles, between B particles, and between particles of a different kind, where r denotes the separation between particles. The correlation function X_ν is related to the fluctuations $N_\nu - \langle N_\nu \rangle$ of the number N_ν of particles of kind ν (ν = A or B) in an arbitrarily chosen volume V according to

$$\langle (N_\nu - \langle N_\nu \rangle)^2 \rangle / \langle N_\nu \rangle = 1 + n_\nu \int_V [X_\nu(r) - 1] \, dV \tag{2}$$

with $\langle N_\nu \rangle = n_\nu V$. The second term on the right-hand side of (2) describes the non-Poissonian spectrum of the density fluctuations. The particles are assumed to be initially ($t = 0$) randomly distributed, i.e. $X_A(r, 0) = X_B(r, 0) = Y(r, 0) = 1$. As the reaction (1) proceeds, the probability of finding particles of a different kind at short distances from each other decreases as a consequence of the reaction $A + B \rightarrow 0$. Thus for small values of r, $Y(r, t)$ becomes smaller than unity. Whether self-organization of the reactants occurs or not depends crucially on the behaviour of the correlation function $X_\nu(r, t)$. An increase of this function at small particle separation indicates local enrichment of

particles of kind ν, i.e. formation of *aggregates*. Since with increasing r the correlations become weaker ($\lim_{r\to\infty} Y=\lim_{r\to\infty} X_\nu=1$), the spatial extension of such aggregates is quite limited.

3. Differential equations for the dynamics of concentrations and correlations

In the following it is assumed that an AB pair disappears spontaneously if the A–B separation becomes equal to or less than a critical value r_0, i.e. we assume $Y(r\leqslant r_0, t)\equiv 0$. (The results obtained in this case agree qualitatively with those for recombination mechanisms involving long-range attractive interactions [20–22], which can be allowed for approximately by a suitable (temperature-dependent) choice of r_0.) The hierarchy of coupled differential equations for the correlation functions of all orders [2] is terminated by using Kirkwood's superposition approximation for the three-particle densities $\rho_{2,1}$ and $\rho_{1,2}$ [34]. For instance, for the three-particle density $\rho_{2,1}$ $(\mathbf{r}_1;\mathbf{r}_2;\mathbf{r}_1^*;t)$, which means the probability that at time t two A-type particles and one B-type particle are located in the volume elements centred at $\mathbf{r}_1$, $\mathbf{r}_2$ and $\mathbf{r}_1^*$, respectively, this approximation reads

$$\rho_{2,1}(\mathbf{r}_1;\mathbf{r}_2;\mathbf{r}_1^*;t)=n_A^2(t)n_B(t)X_A(|\mathbf{r}_1-\mathbf{r}_2|,t)Y(|\mathbf{r}_1-\mathbf{r}_1^*|,t)Y(|\mathbf{r}_2-\mathbf{r}_1^*|,t). \tag{3}$$

This may be readily verified if in Kirkwood's general expression $f(123)=f(12)f(13)f(23)/f(1)f(2)f(3)$ the three-particle distribution function $f(123)$ is identified with $\rho_{2,1}(\mathbf{r}_1;\mathbf{r}_2;\mathbf{r}_1^*;t)$ and if the one-particle and two-particle distribution functions are replaced by the particle concentrations n_A and n_B and the correlation functions X_A and Y with the aid of the following definitions: $f(1)\equiv n_A(t)$, $f(2)\equiv n_A(t)$, $f(3)\equiv n_B(t)$, $X_A(|\mathbf{r}_1-\mathbf{r}_2|,t)\equiv f(12)/f(1)f(2)=f(12)/n_A^2(t)$, $Y(|\mathbf{r}_1-\mathbf{r}_1^*|,t)\equiv f(13)/f(1)f(3)=f(13)/n_A(t)n_B(t)$ and $Y(|\mathbf{r}_2-\mathbf{r}_1^*|,t)\equiv f(23)/f(2)f(3)=f(23)/n_A(t)n_B(t)$.

The Kirkwood approximation gives us the simplest statistical description of the system that involves not only the macroscopic reactant concentrations but also the three correlation functions X_A, X_B and Y, which in previous treatments by the standard chemical-reaction theory [1] had been neglected. However, it is the correlation functions that describe the *spatio–temporal structure* of the system.

As usual, the reaction rate K is defined as the flux of particles B through the surfaces of the recombination spheres with radius r_0 around the particles A, or vice versa. In terms of the dimensionless (primed) quantities $r'=r/r_0$, $t'=(D_A+D_B)t/r_0^2$, $n'_\nu=\gamma_d n_\nu r_0^d$ ($\gamma_d=2$, 2π or 4π for $d=1$, 2 or 3), $D'_\nu=2D_\nu/(D_A+D_B)$, $K'\equiv(\partial Y/\partial r')_{r'=1}=K/\gamma_d(D_A+D_B)r_0^{d-2}$, the equations governing the present model read

$$\frac{dn'_A}{dt'}=\frac{dn'_B}{dt'}=-K'n'_An'_B \tag{4}$$

$$\frac{\partial X_\nu(r',t')}{\partial t'}=D'_\nu\Delta X_\nu-2K'X_\nu n'_\mu J_d[Y] \qquad \nu=\text{A or B} \qquad \mu=\text{B or A} \tag{5}$$

$$\frac{\partial Y(r',t')}{\partial t'}=\Delta Y-K'Y\sum_\nu^{A,B} n'_\nu J_d[X_\nu]. \tag{6}$$

The functionals $J_d[Z]$ with $Z=X_A, X_B$ or Y are d-dependent [2]. For $d=1$, 2 and 3 we have

$$J_1[Z]=\tfrac{1}{2}[Z(|r'-1|)+Z(r'+1)-2] \tag{7a}$$

$$J_2[Z]=\frac{1}{\pi}\int_{-1}^{+1}\frac{[Z(\phi)-1]\,d\xi}{(1-\xi^2)^{1/2}} \qquad \text{with } \phi=(r'^2+2r'\xi+1)^{1/2} \tag{7b}$$

$$J_3[Z]=\frac{1}{2r'}\int_{|r'-1|}^{r'+1}(Z(\xi)-1)\xi\,d\xi \tag{7c}$$

respectively.

Equations (5) and (6) for the *correlation dynamics* complement (4) for the *concentration dynamics*. This is in contrast to the traditional approach, generally accepted until about two decades ago, in which $X_\nu \equiv 1$ was assumed to hold at *any* time and for *any* initial distribution $Y(r, t=0)$. The underlying assumption of Poisson distributions for particles of the same kind seemed to be justified since, in the absence of interactions between particles of the same kind, there was no easily recognizable reason for them not to be and to remain distributed at random. In this approximation [1, 35, 36] the correlation dynamics is governed by a *linear* equation for Y. In the case $d=3$ the reaction rate K reaches its steady-state value $4\pi(D_A+D_B)r_0$ after a transition period of the order of magnitude $r_0^2/(D_A+D_B)$.

However, the nonlinear terms in (4) to (6) introduce many-particle effects which are in conflict with the simple picture just outlined:

(i) The reaction rate K mediately depends on the spatial correlations between particles of the same kind. Its time dependence will therefore be different from that predicted by the rate-equation approach.

(ii) As a result of the boundary condition imposed on Y (i.e. A–B recombination at $r \leqslant r_0$), a (positive) source term appears on the right-hand side of (5).

(iii) As a consequence of the effect of (ii) on $X_\nu(r)$, equation (6) contains an additional (negative) sink term, and so on.

The nonlinear coupling terms amplify, by feedback, the changes in $Y(r)$ originally induced by the reaction $A+B \rightarrow 0$. In the course of time this leads to significant deviations of the density fluctuations $X_\nu(r)$ from the Poisson distribution.

4. Results and discussion

In the remainder of this paper numerical solutions of (4) to (6) for various reactant mobilities and space dimensions will be compared with results obtained from standard chemical-kinetics treatments, in which, as explained above, the many-particle effects were neglected.

Figure 1 shows the decay of the particle concentrations $n_A(t)=n_B(t)\equiv n(t)$ for $d=1$ and different initial concentrations $n(0)$. The larger $n(0)$, the earlier deviate the solutions of (4) to (6) from the standard results [1, 35] based on (4) with $K=4\pi D r_0[1+r_0/(\pi D t)^{1/2}]$ and $D=D_A+D_B$. For $\kappa=1$ the decay is slightly slower than for $\kappa=0$. There is good agreement with two recent independent computer simulations [18, 19], the result of which for $n'(0)=0.4$ is included in figure 1.

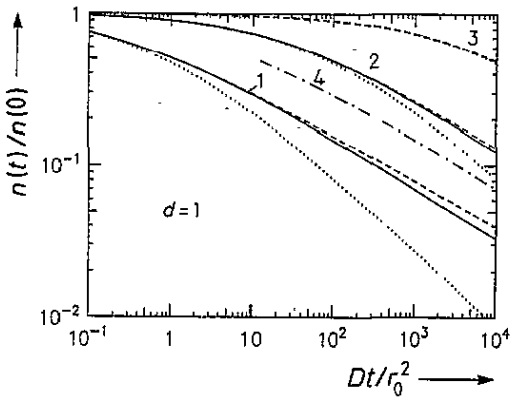

Figure 1. Decay of the concentration n as a function of time t for $d=1$. The curve families 1, 2 and 3 correspond to initial concentrations $n'(0)=1$, 0.1 and 0.01, respectively. Curve 4 shows the result of a computer simulation for $n'(0)=0.4$ [19]. Solid and broken lines represent the cases $D_A=0$, $D_B>0$ and $D_A=D_B$, respectively; dotted lines show the results of standard chemical kinetics.

As in the description of critical phenomena it is useful to introduce the *critical exponent*

$$\alpha(t)=-\frac{\mathrm{d}\ln n'(t')}{\mathrm{d}\ln t'}=-\frac{\mathrm{d}\ln n(t)}{\mathrm{d}\ln t}=Kn(t)t. \tag{8}$$

According to estimates of Ovchinnikov and Zeldovich [10] as well as others [37, 38], its limiting value for $t\to\infty$ is given by $\alpha(\infty)=d/4$, which has to be compared with the classical values of $\frac{1}{2}$, 1 and 1 for $d=1$, 2 and 3, respectively. Thus, for example, for $d=1$ the fluctuation-controlled value of $\alpha(\infty)$ is smaller by a factor of 2 than the 'classical' value. As seen in figure 2, the higher $n(0)$ the faster approaches α its asymptotic value. For immobile reactants A, $\alpha(t)$ is systematically higher than in cases of equal mobilities

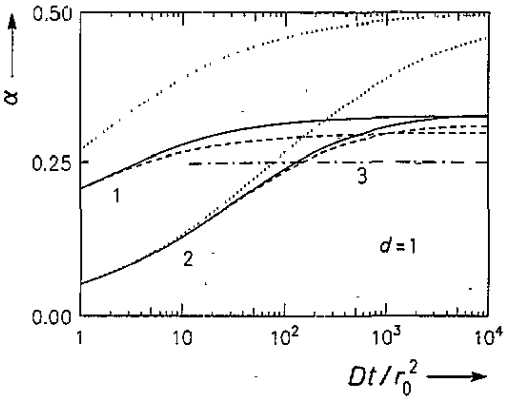

Figure 2. Critical exponents α as functions of time t for $d=1$. The curve families 1 and 2 belong to initial concentrations $n'(0)=1$ and 0.1, respectively. Curve 3 shows the result of a computer simulation [19]. Solid and broken lines represent the cases $D_A=0$, $D_B>0$ and $D_A=D_B$, respectively; dotted lines show the results of standard chemical kinetics.

of A- and B-type particles. This corresponds to the faster concentration decay rates for immobile A-type particles illustrated in figure 1.

The temporal evolution of *spatial correlations* in the case $d=1$ is shown in figures 3(a) and 3(b) for the limiting cases $\kappa=1$ and $\kappa=0$. A striking feature is the rapid

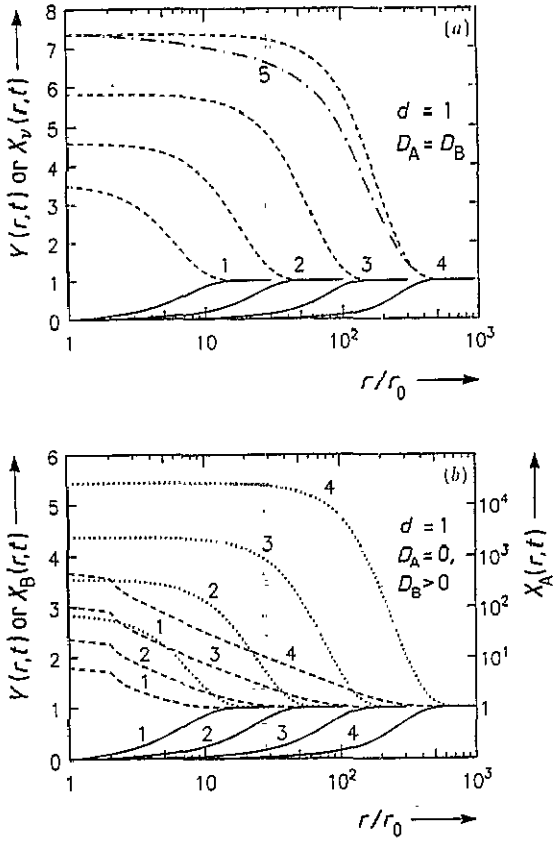

Figure 3. Correlation functions for particles of the same kind, X_ν with $\nu=$ A or B (broken or dotted curves), and of different kind, Y (solid curves), versus the (logarithmically plotted) particle distance r for $d=1$ and initial concentration $n'(0)=1$. Figure 3(a) shows the case $D_A=D_B$; in figure 3(b) ($D_A=0$, $D_B>0$) the right-hand scale belongs to the broken curves. The curves labelled 1–4 refer to $t'=10^1$, 10^2, 10^3 and 10^4, respectively. Curve 5 in figure 3(a) is the result of a computer simulation [17].

growth of the non-Poissonian density fluctuations of particles of the same kind for decreasing values of r/r_0. For example, for $t=10^4r_0^2/D$ and $\kappa=1$ the probability density of finding a close A–A or B–B pair exceeds that of a random distribution by more than a factor of 7. This prediction may be used as a suitable criterion for the occurrence of aggregation in studies of reactions between defects in solids. In particular, this was used to demonstrate the formation of clusters of F centres in KCl crystals after long-time X-ray irradiation at 4K [25]. In this case the concentrations of monomer, dimer and trimer F centres (formed by anion vacancies on nearest to third-nearest-neighbour sites that have captured 1 to 3 electrons, respectively) can be measured by optical absorption [39]. (The *shape of extended clusters or domains* of F centres becomes trapezoidal (figure 3(a)), in agreement with both computer simulations and theory [17].) Information on

the *density and compactness of clusters* follows from figure 3(*b*): For $\kappa = 0$, the immobile particles A form denser and more compact clusters than the mobile B particles.

Figures 3(*a*) and 3(*b*) demonstrate further that at long reaction times the characteristic reaction scale, the recombination radius r_0 (determining the steady-state reaction rate K in the standard chemical kinetics [1]), is replaced by a new scale of the order of magnitude of the diffusion length $(Dt)^{1/2}$ [34]. This plays the role of a *correlation length* determining the distinctive size of A- or B-rich domains and corresponding to the distance below which both types of correlation functions, Y and X_ν, deviate from the Poisson distribution considerably. As shown earlier [32], for $t \to \infty$ the correlation functions for particles of the same kind may be analytically described by

$$X_\nu - 1 \propto (\ln t)^2 \exp(-r^2/4D_\nu t). \tag{9}$$

This is confirmed by both the present calculations and recent computer simulations [17].

The results of (4) to (6) for $d=2$ are not presented here, since they are quite similar to those for $d=3$ shown in figures 4 and 5. Compared with $d=1$, in the case $d=3$ the concentrations decay much faster (figure 4(*a*)), with $\alpha(\infty)=\frac{1}{2}$ for $\kappa=0$ [33], $\alpha(\infty)=\frac{3}{4}$ for $\kappa=1$ and $\alpha(\infty)=1$ in the standard rate-equation treatment (figure 4(*b*)). Moreover,

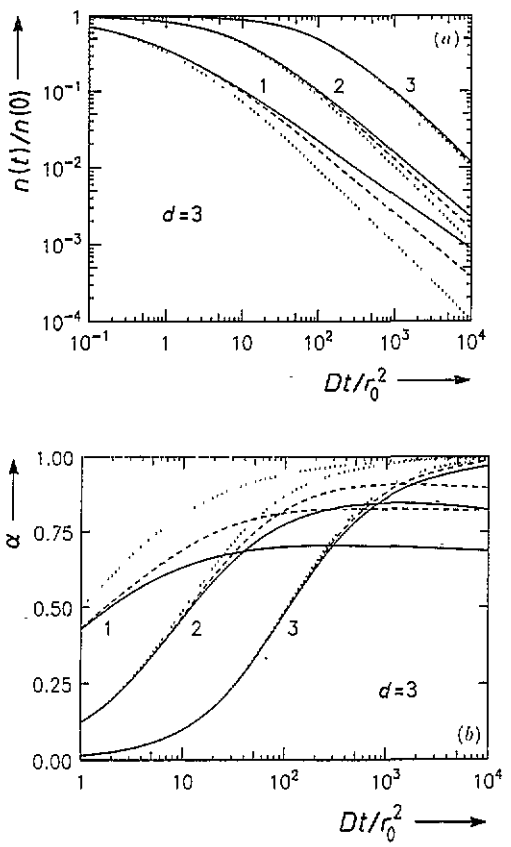

Figure 4. Concentration n (figure 4(*a*)) and critical exponent α (figure 4(*b*)) as functions of time t for $d=3$. The curve families 1, 2 and 3 correspond to initial concentrations $n'(0) = 1$, 0.1 and 0.01, respectively. Solid and broken lines represent the cases $D_A = 0$, $D_B > 0$ and $D_A = D_B$, respectively; dotted lines show the results of standard chemical kinetics.

the difference in $n(t)$ for $\kappa=0$ and $\kappa=1$ grows much faster for $d=3$ than for $d=1$. Therefore, as predicted earlier [18], the effect of the relative mobilities of the particles A and B is more pronounced and thus more easily recognizable in computer simulations for $d=3$ than for $d=1$. On the other hand, fluctuation effects (which are responsible for the non-standard kinetics) are less pronounced for $d=3$. As a consequence, ascertaining significant deviations from the kinetics predicted by the linear theory and, *a fortiori*, establishing the numerical values of $\alpha(\infty)$ requires much longer reaction times for $d=3$ (figure 4(*b*)) than for $d=1$ (figure 2). Preliminary computer simulations [40] for $d=3$ have given α values of 0.79 for $\kappa=1$ and 0.69 for $\kappa=0$, which means that the simulations must be extended to much larger $n(0)/n$ values in order to obtain α values that are close to the limiting values $\alpha(\infty)=0.75$ and 0.50.

With regard to the spatial distribution of mobile particles figures 5(*a*) and (*b*) show the following:

(i) The deviations from the Poisson distribution are much smaller for $d=3$ than for $d=1$ (e.g. for $\kappa=1$, $X_v(r'\to 0, t'=10^4)\approx 3$ or 7, respectively).

(ii) As for $d=1$, $(Dt)^{1/2}$ is the characteristic length determining the size of A- or B-rich domains.

(iii) The gap between alternating domains of particles of a different kind is less pronounced for $d=3$ than for $d=1$. While for $d=1$ the correlation function Y, whose time behaviour was studied in detail by Leyvraz and Redner [17], is practically equal to zero up to a certain distance before it abruptly increases (figure 3), for $d=3$ a long tail reaches down to short distances and thus smooths the step (figure 5).

The principal results of the present Letter may be summarized as follows:

(a) It has been demonstrated by a microscopic approach based on the use of correlation functions that even the simplest bimolecular reaction, the annihilation reaction $A+B\to 0$, may give rise to spatial self-organization.

(b) The kinetics of the reaction $A+B\to 0$ depends not only on the spatial dimension d of the system as predicted by standard rate-equation theory but also on the diffusivity ratio D_A/D_B and the initial concentrations $n_A(t=0)$ and $n_B(t=0)$.

(c) Extensive investigations [2–4] of the manifestation of self-organization in the reaction $A+B\to 0$ under a variety of conditions (mobile and immobile reactants, contact or long-range recombination, presence or absence of a permanent particle source) have led us to the conclusion that in this reaction self-organization is a *universal phenomenon*, the driving force being the annihilation itself.

(d) The good agreement of the present approach with computer simulations may be taken as a justification of the use of Kirkwood's superposition approximation (3), which allowed us to obtain (5) and (6) in addition to the rate equation (4). In this approach the equations (4) for the concentrations n_A and n_B are coupled to the correlation dynamics (equations (5) and (6)) through a time-dependent reaction rate K.

Finally, the present work sheds new light on the so-called Hanusse–Light–Tyson theorem [41] widely used in synergetics. This theorem claims that a limiting cycle (auto-oscillating regime) cannot occur in a system with two intermediate products if the only reactions taking place are mono- and bimolecular ones. An analysis of the simplest two-stage processes, namely the Lotka and the Lotka–Volterra models formulated to include diffusion control by methods analogous to those presented above, has shown that the theorem is not tenable [2, 42]. Since the reacion rate K depends on the density fluctuations (as in the present work), there are reaction regimes in which the correlation dynamics dominate over the concentration dynamics. Under these circumstances a formal analysis based on bifurcation theory is bound to fail.

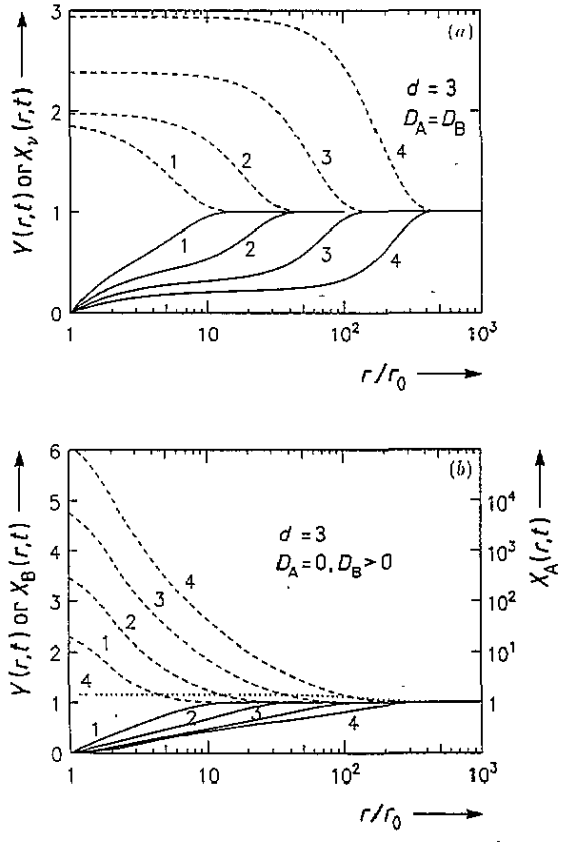

Figure 5. Correlation functions for particles of the same kind, X_ν with $\nu = A$ or B (broken or dotted curves), and of different kind, Y (solid curves), versus the (logarithmically plotted) particle distance r for $d = 3$ and initial concentration $n'(0) = 1$. Figure 5(*a*) shows the case $D_A = D_B$; in figure 5(*b*) ($D_A = 0$, $D_B > 0$) the right-hand scale belongs to the broken curves. The curves labelled 1–4 refer to $t' = 10^1$, 10^2, 10^3 and 10^4, respectively. Note that in the case $D_A = 0$, $D_B > 0$ for these t' values the X_B curves practically coincide with the curve $X_B(t' = 10^4)$ shown in figure 5(*b*) as the dotted curve 4.

Acknowledgments

The authors are very grateful to A Blumen, A Ovchinnikov, S Redner, I Sokolov and M Zaiser for numerous stimulating discussions. E Kotomin thankfully acknowledges financial support by the Max-Planck-Gesellschaft, which made this collaboration possible, and the hospitality experienced during his stay at the Institut für Physik of the Max-Planck-Institut für Metallforschung in Stuttgart.

References

[1] Eyring H, Lin S H and Lin S M 1980 *Basic Chemical Kinetics* (New York: Wiley)
[2] Kuzovkov V and Kotomin E 1988 *Rep. Progr. Phys.* **51** 1497; 1992 *Rep. Progr. Phys.* **55** 2079
[3] Special issue of *J. Stat. Phys.* 1991 *J. Stat. Phys.* **65** no 5/6
[4] Vinetsky V, Kalnin Yu, Kotomin E and Ovchinnikov A 1990 *Sov. Phys. Usp.* **33** 793

[5] Kubin L P and Martin G (eds) 1988 *Non-Linear Phenomena in Materials Science* (Aedermannsdorf: Trans Tech Publications)
[6] Seeger A 1989 *Rad. Effects Defects in Solids* **111/112** 355
[7] Hähner P and Frank W 1992 *Solid State Phenomena* **23/24** 203
[8] Zaiser M, Frank W and Seeger A 1992 *Solid State Phenomena* **23/24** 221
[9] Song S and Poland D 1992 *J. Phys. A: Math. Gen.* **25** 3913
[10] Ovchinnikov A A and Zeldovich Ya B 1978 *Chem. Phys.* **28** 215
[11] Zeldovich Ya B and Mikhailov A S 1989 *Sov. Phys.-Usp.* **30** 977
[12] Mikhailov A S 1989 *Phys. Rep.* **184** 302
[13] Davydov V A, Zykov V S and Mikhailov A S 1991 *Sov. Phys.-Usp.* 34 665
[14] Haken H 1978 *Synergetics* (Berlin: Springer)
[15] Haken H 1984 (ed) *Chaos and Order in Nature* (Berlin: Springer)
[16] Zhabotinsky A M 1974 *Concentration Auto-Oscillations* (Moscow: Nauka)
[17] Leyvraz F and Redner S 1991 *Phys. Rev. Lett.* **66** 2168
[18] Solokov I M, Schnörer H and Blumen A 1991 *Phys. Rev.* A **44** 2388
[19] Argyrakis P and Kopelman R 1992 *Phys. Rev.* A **45** 5814
[20] Schnörer H, Kuzovkov V and Blumen A 1989 *Phys. Rev. Lett.* **63** 805
[21] Schnörer H, Kuzovkov V and Blumen A 1990 *J. Chem. Phys.* **92** 2310; 1990 *J. Chem. Phys.* **93** 7148
[22] Luding S, Schnörer H, Kuzokov V and Blumen A 1991 *J. Stat. Phys.* **65** 1261
[23] Lück G and Sizmann R 1964 *Phys. Status Solidi* **6** 263; 1966 *Phys. Status Solidi* **14** 507
[24] Tale I, Millers D and Kotomin E 1975 *J. Phys. C: Solid State Phys.* **8** 2366
[25] Kuzovkov V and Kotomin E 1984 *J. Phys. C: Solid State Phys.* **17** 2283
[26] Jin N Y, Phillipp F and Seeger A 1989 *Phys. Status Solidi* A **116** 91
[27] Kuzovkov V and Kotomin E 1993 *Phys. Scripta* 47 585
[28] Zhang Y-C 1987 *Phys. Rev. Lett.* **59** 1726
[29] Lindenberg K, West B J and Kopelman R 1988 *Phys. Rev. Lett.* **60** 1777
[30] Kanno S 1988 *Prog. Theor. Phys.* 79 721 & 1330
[31] Martin G 1975 *Phil. Mag.* **32** 615
[32] Kuzovkov V and Kotomin E 1983 *Chem. Phys.* **76** 479; **81** 335
[33] Kotomin E and Kuzovkov V 1985 *Chem. Phys. Lett.* **117** 266
[34] Balescu R 1975 *Equilibrium and Non-Equilibrium Statistical Mechanics* (New York: Wiley)
[35] Waite T R 1957 *Phys. Rev.* **107** 463
[36] Leibfried G 1965 *Bestrahlungseffekte in Festkörpern* (Stuttgart: Teubner)
[37] Kang K and Redner S 1984 *Phys. Rev. Lett.* 52 955; 1985 *Phys. Rev.* A **32** 435
[38] Zumofen G, Blumen A and Klafter J 1985 *J. Chem. Phys.* **82** 3198
[39] Stoneham A M 1975 *Theory of Defects in Solids* (Oxford: Clarendon)
[40] Vitukhnovsky A G, Pyttel B L and Sokolov I M 1988 *Phys. Lett.* A **128** 161; 1987 *Phys. Inst. Acad. of Sciences of the USSR* No. 58
[41] Hanusse P 1972 *C. R. Acad. Sci. Paris* C **274** 1245
Tyson J and Light J 1973 *J. Chem. Phys.* 59 4164
[42] Kuzovkov V 1991 *Proc. Latv. Acad. Sci. Phys.* no 2, p 3